



Get Clarity On Generics

Cost-Effective CT & MRI Contrast Agents



FRESENIUS
KABI

WATCH VIDEO

AJNR

Metachromatic Leukodystrophy: Diffusion MR Imaging Findings

R. Nuri Sener

AJNR Am J Neuroradiol 2002, 23 (8) 1424-1426

<http://www.ajnr.org/content/23/8/1424>

This information is current as
of August 7, 2025.

Case Report

Metachromatic Leukodystrophy: Diffusion MR Imaging Findings

R. Nuri Sener

Summary: Herein the case of a 10-month-old boy with metachromatic leukodystrophy is reported. Diffusion MR imaging performed with an echo-planar trace sequence revealed a cytotoxic edema-like pattern (high signal intensity on $b = 1000 \text{ s/mm}^2$ images and low apparent diffusion coefficient values) in the affected white matter in the absence of an ischemic condition. This finding was unchanged at a 6-month follow-up, as revealed by diffusion MR imaging. A gradient-echo diffusion sequence, reverse fast imaging in steady-state precession, revealed hyperintense changes at the corresponding regions. It is likely that the cytotoxic edematous pattern (restricted diffusion pattern) reflected restriction of mobility of the water molecules within abnormal portions of the myelin sheath, because impaired myelin breakdown and reutilization are known features of metachromatic leukodystrophy.

Metachromatic leukodystrophy is caused by a deficiency of arylsulfatase-A resulting in impaired myelination (1–8). Diffusion MR imaging features of the condition have not been reported previously. We report diffusion MR imaging of metachromatic leukodystrophy performed by using the echo-planar and gradient-echo sequences.

Case Report

The patient was a 10-month-old boy presenting with progressive spasticity. An MR imaging examination was performed on a 1.5-T MR unit (Magnetom Vision; Siemens, Erlangen, Germany) with a gradient strength of 30mT/m. T2-weighted images revealed hyperintense changes, mainly involving the deep white matter, and atrophy (Fig 1A). Diffusion MR imaging was performed by using the echo-planar trace sequence (5700/139 [TR/TE]; acquisition time, 22 s) with averaging of the three gradients. On $b = 1000 \text{ mm}^2/\text{s}$ images, which were heavily diffusion-weighted images, hyperintense changes were evident in the deep white matter and had a signal intensity pattern similar to that of cytotoxic edema (Fig 1B). On automatically generated apparent diffusion coefficient (ADC) maps, the ADC values obtained by region of interest evaluations were low at the corresponding regions (eg, $0.55 \times 10^{-3} \text{ mm}^2/\text{s}$), compared with the peripheral regions of the parenchyma (eg, $0.95 \times 10^{-3} \text{ mm}^2/\text{s}$) (Fig 1C).

A diagnosis of metachromatic leukodystrophy was confirmed by revealing decreased activity of arylsulfatase-A in

leukocytes and increased urinary sulfatides. After 6 months, the patient was reexamined by diffusion MR imaging. The same echo-planar trace sequence was used, and hyperintense changes were again observed on $b = 1000 \text{ mm}^2/\text{s}$ images (Fig 2A), as were low ADC values in the deep white matter. A gradient-echo diffusion sequence, the reverse fast imaging in steady-state precession sequence, was obtained at the same session. For the reverse fast imaging in steady-state precession sequence (21.6/5 [TR/TE]; acquisition time, 2 min 48 s), high pixel values were evident in the deep white matter, compared with the peripheral regions of the parenchyma (Fig 2B). (ADC value calculation is not possible with reverse fast imaging in steady-state precession.)

Discussion

It has been reported that in cases of metachromatic leukodystrophy, the decreased activity of arylsulfatase-A accounts for failure of myelin breakdown and reutilization; hence, dysmyelination (1–8). On the diffusion MR images in the current case of metachromatic leukodystrophy, a cytotoxic, edematous pattern (restricted diffusion pattern) was evident in the deep white matter in the absence of an ischemic condition. The distribution of the lesions (Fig 1B) and their unchanging pattern on 6-month follow-up diffusion MR images (Fig 2A) strongly suggested that the lesions were directly related to the disease process. Restricted diffusion was manifested by hyperintense changes on heavily diffusion-weighted ($b = 1000 \text{ s/mm}^2$) images (Fig 1B) and low ADC values (eg, $0.55 \times 10^{-3} \text{ mm}^2/\text{s}$) on ADC maps (Fig 1C) of the echo-planar trace sequence. In addition, on the gradient-echo diffusion-weighted images, obtained using reverse fast imaging in steady-state precession, high signal intensity and high pixel values were evident in the deep white matter (Fig 2B) and were similar to those seen on $b = 1000 \text{ s/mm}^2$ images, which again indicated definite abnormality in these regions. However, absolute ADC value calculation is currently not possible with the reverse fast imaging in steady-state precession sequence.

A similar diffusion MR imaging pattern on echo-planar diffusion images of patients with phenylketonuria was recently reported by Phillips et al (9). In that study, patients with phenylketonuria had highly restricted diffusion of water molecules with high signal intensity of the white matter on $b = 1000 \text{ s/mm}^2$ images in association with low ADC values on ADC maps (between 0.56 and $0.63 \times 10^{-3} \text{ mm}^2/\text{s}$) (9). The authors concluded that this restricted diffusion pattern in cases of phenylketonuria reflected impaired myelination, and protons within partially that de-

Received December 5, 2001; accepted after revision May 1, 2002.

Department of Radiology, Ege University Hospital, Bornova, Izmir, Turkey.

Address reprint requests to R. Nuri Sener, MD, Professor of Radiology, Department of Radiology, Ege University Hospital, Bornova, Izmir, Turkey.

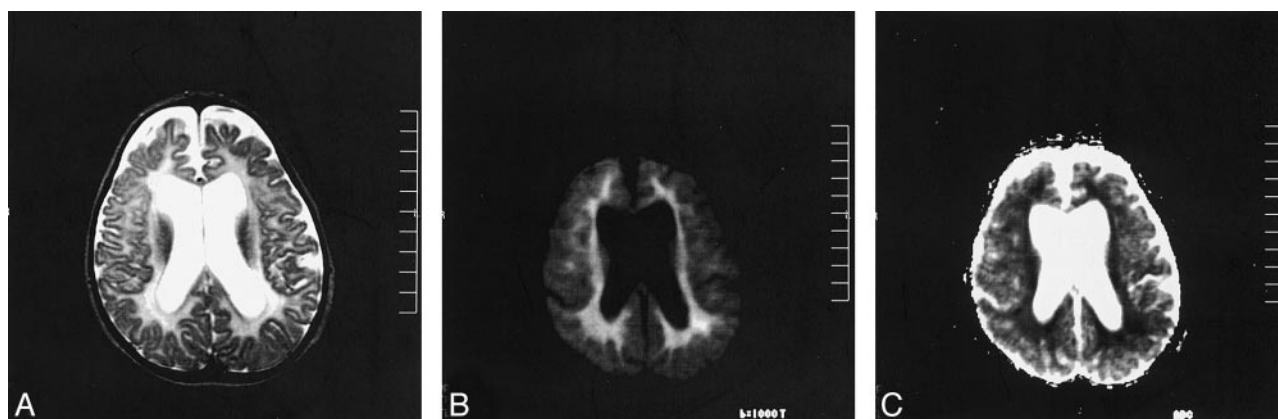


FIG 1. Images obtained at initial examination, performed when the patient was 10 months old.

A, T2-weighted image reveals hyperintense changes in the deep white matter and atrophy.

B, A $b = 1000 \text{ mm}^2/\text{s}$ (heavily diffusion-weighted) image from an echo-planar trace sequence reveals hyperintense changes similar to those of cytotoxic edema.

C, Corresponding ADC map reveals a low signal intensity and low ADC value ($0.55 \times 10^{-3} \text{ mm}^2/\text{s}$) in the deep white matter compared with the peripheral regions of the parenchyma, including peripheral white matter and the cortex ($0.95 \times 10^{-3} \text{ mm}^2/\text{s}$).

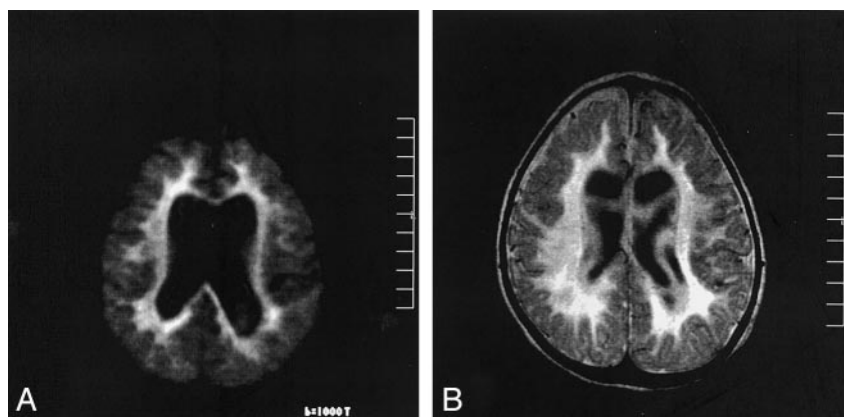


FIG 2. Images obtained during follow-up, when the patient was 16 months old.

A, A $b = 1000 \text{ mm}^2/\text{s}$ (heavily diffusion-weighted) image from an echo-planar trace sequence reveals same hyperintense lesions.

B, Gradient-echo diffusion sequence (reverse fast imaging in steady-state precession) reveals high signal intensity and high pixel values (165) in the deep white matter, compared with the peripheral regions of the parenchyma (99).

stroyed portions of the myelin sheath may not be as mobile as those in normal parenchyma (9). On the other hand, in a recent experiment, Branco (10) showed that transition of water from the solid to the gel state contributes to the signal intensity on diffusion MR images, and in the gel state, high signal intensity is observed on $b = 1000 \text{ s}/\text{mm}^2$ images (this should result in low ADC values). Considering the observations by Phillips et al (9) and the experiment by Branco (10), in the current case of metachromatic leukodystrophy, the restricted diffusion pattern probably was consistent with some disintegration of the white matter secondary to impaired myelination, and restriction of mobility of the water molecules within abnormal portions of myelin sheath resulted in a diffusion MR imaging pattern similar to that of cytotoxic edema.

Conclusion

In a case of metachromatic leukodystrophy, an echo-planar trace sequence revealed a cytotoxic edematous pattern (restricted diffusion pattern) in the deep white matter in the absence of an ischemic condition. This pattern, manifested by high signal

intensity on $b = 1000 \text{ s}/\text{mm}^2$ images and low ADC values, probably reflected restriction of mobility of the water molecules within abnormal portions of the myelin sheath, considering that impaired myelin breakdown and reutilization are known features of metachromatic leukodystrophy. Hence, dysmyelination is a feature of metachromatic leukodystrophy. A gradient-echo diffusion sequence, reverse fast imaging in steady-state precession, revealed hyperintense changes at the corresponding regions similar to those seen on $b = 1000 \text{ s}/\text{mm}^2$ images. Further diffusion MR imaging studies of dysmyelinating disorders could contribute to our understanding of the imaging properties of these diseases.

References

1. Barkovich AJ. Concepts of myelin and myelination in neuroradiology. *AJNR Am J Neuroradiol* 2000;21:1099-1109
2. Faerber EN, Melvin J, Smergel EM. MRI appearances of metachromatic leukodystrophy. *Pediatr Radiol* 1999;29:669-672
3. Kim TS, Kim IO, Kim WS, et al. MR of childhood metachromatic leukodystrophy. *AJNR Am J Neuroradiol* 1997;18:733-738
4. Kaye EM. Update on genetic disorders affecting white matter. *Pediatr Neurol* 2001;24:11-24
5. Johannsen P, Ehlers L, Hansen HJ. Dementia with impaired tem-

- poral glucose metabolism in late-onset metachromatic leukodystrophy. *Dement Geriatr Cogn Disord* 2001;12:85–88
6. Felice KJ, Gome Zlira M, Natowicz M, et al. **Adult-onset MLD: a gene mutation with isolated polyneuropathy.** *Neurology* 2000;55:1036–1039
 7. Bostantjopoulou S, Katsarou Z, Michelakaki H, Kazis A. **Seizures as a presenting feature of late onset metachromatic leukodystrophy.** *Acta Neurol Scand* 2000;102:192–195
 8. Mancini GM, van Diggelen OP, Huijman JG, Stroink H, de Co
RF. **Pitfalls in the diagnosis of multiple sulfatase deficiency.** *Neuropediatrics* 2001;32:38–40
 9. Phillips MD, McGraw P, Lowe MJ, Mathews VP, Hainline BE. **Diffusion-weighted imaging of white matter abnormalities in patients with phenylketonuria.** *AJNR Am J Neuroradiol* 2001;22:1583–1586
 10. Branco G. **An alternative explanation of the origin of the signal in diffusion-weighted MRI.** *Neuroradiology* 2000;42:96–98